Rapid prototyping based on variable polarity gas tungsten arc welding for a 5356 aluminium alloy

H Wang and **R Kovacevic***
Research Center for Advanced Manufacturing, Southern Methodist University, Richardson, Texas, USA

Abstract: This paper presents a new deposition process for directly building cylindrical parts of the 5356 aluminium alloy with variable polarity gas tungsten arc welding (VPGTAW). The relationship between the geometric sizes of the deposited layer and the welding parameters is investigated. A machine vision sensor is used to monitor and control the arc length that is a key welding parameter in the achievement of a uniform deposition. By optimizing the depositing speed and the thickness of the depositing layer, there is no need for a cooling system to cool the part. Three-dimensional parts with different wall thicknesses and different shapes are successfully obtained. The surfaces of the deposited parts are smooth and uniform.

Keywords: rapid prototyping, aluminium part, variable polarity gas tungsten arc welding

1 INTRODUCTION

One challenge for rapid prototyping (RP) is to develop the capability to create directly functional metallic parts that are dense, metallurgically bonded, geometrically accurate and have a good surface appearance. A weld-based RP is one of the techniques that offers a promising approach to satisfy the requirements of this challenge.

The use of welding to create free-standing shapes was established in Germany in the 1960s [**1**]. Companies such as Krupp, Thyssen and Sulzer developed welding techniques for the fabrication of large components of simple geometry such as pressure vessels that can weigh up to 500 t [**2**]. Other work in this area was undertaken by Babcock and Wilcox [**3**] who worked mainly on large components produced in an austenitic material. Also, at the beginning of the 1990s, work by Rolls–Royce (Manufacturing Technology Section, Rolls–Royce Aerospace Group, Bristol, personal communication) centred on investigating the technique as a means of reducing the waste levels of expensive, high-performance alloys that can occur in conventional processing. Rolls–Royce successfully produced various aircraft engine parts in nickel-based and titanium-based alloys. Research work on the weld-based RP continues at the University of Nottingham, UK [**4**], the University of Minho, Portugal, the University of Wollongong, Australia [**5**–**7**], and Southern Methodist University, United States [**8**, **9**]. Two new research groups, one from Korea [**10**] and the other consisting of researchers from the Indian Institute of Technology, Bombay, and the Fraunhofer Institute of Production Technology and Automation [**11**], presented their conceptual ideas of combining a welding operation with milling. The Korean research group proposed to combine welding and five-axis computer numerically controlled (CNC) milling for the direct prototyping of metallic parts. The other research group from Germany and India proposed to combine welding with 2.5-axis milling, where the complex shapes of the layers are obtained by using cutters with specific geometry. The brazing process is proposed to deposit the masking material at the edge of each layer in order to allow the formation of an overhang [**11**].

It is important to note that all of the above research work focuses on the rapid prototyping of parts made of steel. However, aluminium alloys also have a widespread history of applications in the industry. Therefore, the development of a rapid prototyping technique for building functional parts from aluminium alloys is needed.

2 EXPERIMENTAL PROCEDURE

2.1 VPGTAW process

Gas tungsten arc welding (GTAW) is an arc-welding process that uses an arc between a tungsten electrode

The MS was received on 12 October 2000 and was accepted after revision for publication on 26 March 2001.
**Corresponding author: Research Center for Advanced Manufacturing, Southern Methodist University, 1500 International Parkway, Suite 100, Richardson, TX 75081, USA.*

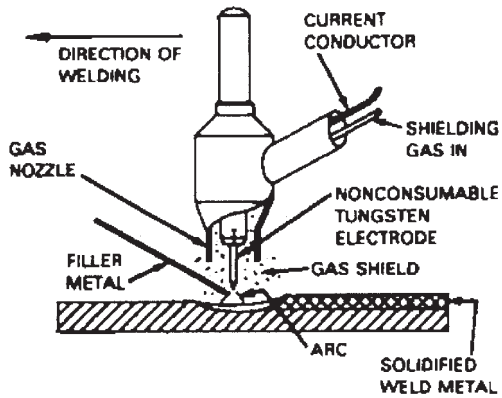

Fig. 1 Gas tungsten arc welding operation

(non-consumable) and the material to be welded. Figure 1 shows the principle of the GTAW process. The process uses a tungsten, or tungsten alloy, electrode held in a torch. Shielding gas is fed through the torch to protect the electrode, the molten pool and the solidified weld metal from contamination by the atmosphere. The electric arc is produced by the passage of current through the conductive, ionized shielding gas. The arc is established between the tip of the electrode and the work. Heat generated by the arc melts the base metal. Once the arc and molten pool are established, the torch is moved along the joint and the arc progressively melts the faying surfaces. Filler wire, if used, is usually added to the leading edge of the molten pool to fill the joint. Compared with laser and gas metal arc welding, some selected advantages of GTAW [**12**] as a technique for rapid prototyping are as follows:

1. It can use relatively inexpensive power supplies.
2. It is free of spatter.
3. It allows precise control of welding variables.
4. It allows the heat source and filler metal additions to be controlled independently.

Variable polarity GTAW is an ideal arc welding process for aluminium alloys. Using direct current, the tungsten electrode may be connected to the negative, direct current electrode negative (DCEN) polarity, or the positive terminal of the power supply, direct current electrode positive (DCEP) polarity. When the electrode polarity is DCEP, a cathodic cleaning action is created at the surface of the workpiece. This action occurs with most metals but is most important when welding aluminium and magnesium because it removes the refractory oxide surface that inhibits wetting of the weldment by the weld metal. In contrast to DCEN polarity, where the electrode tip is cooled by the evaporation of electrons, in DCEP polarity when the electrode is used as the positive pole, its tip is heated by the bombardment of electrons as well as by its resistance to their passage through the electrode. Therefore, in DCEP polarity, the burning of the electrode tip is a serious problem. It is well known that the shape of the tungsten electrode tip is an important process variable in GTAW. It is important that a consistent electrode geometry be used once a welding procedure is established.

The key to the variable polarity technique is that the duration and magnitude of the DCEN and DCEP current excursions can be controlled separately. The typical waveform of the variable polarity current is shown in Fig. 2. The DCEP current amplitude is greater than the DCEN current amplitude but the DCEP time is much shorter than the DCEN time. The added DCEP current provides an additional spike of cleaning action to break up the surface oxides on the workpiece yet produces a minimum of heat input on the electrode. An appropriate cleaning of the weld face and root face can be accomplished by increasing the DCEP current by an additional 30–80 A.

2.2 Experimental set-up

The developed experimental rapid prototyping system is shown in Fig. 3. The VPGTAW technology is used to build parts of 5356 aluminium alloy; the diameter of the feed wire is 1.2 mm. There are two vertical axes, the Z axis and Z' axis. The Z' axis is fixed to the Z axis, and the welding torch is attached to the Z' axis. The Z axis moves up continuously at a constant speed during the deposition process and this continuous movement produces a smoother surface than could otherwise be achieved. The moving speed of the Z axis depends on

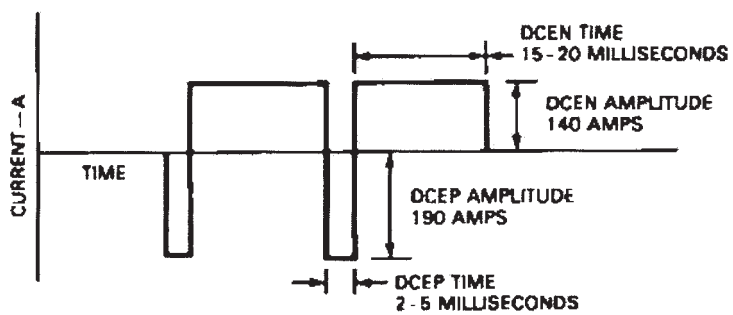

Fig. 2 Typical variable polarity current waveform

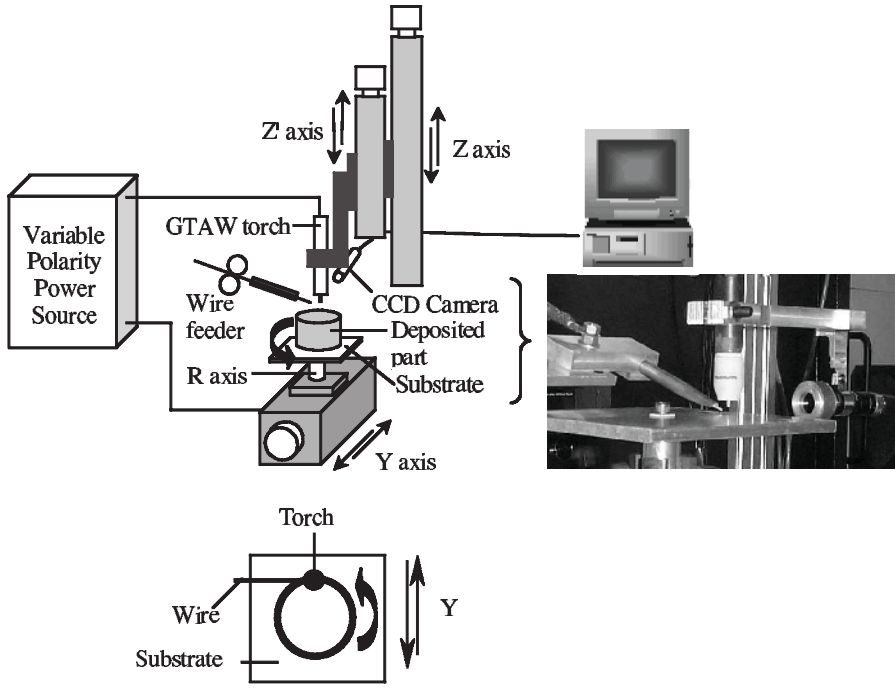

Fig. 3 Schematic diagram of the experimental set-up

the substrate rotating speed and the deposition layer height. The movement of the Z' axis is controlled to provide a constant arc length during the deposition process according to the acquired arc length signal. The arc length is monitored in real time by a machine-vision system consisting of a charge-coupled device (CCD) camera, an arc-light filter and an image processing system. The CCD camera is attached to the torch with a small bracket. The three-dimensional part is built on a substrate that is fixed on a rotating axis, the R axis. The R axis is attached to the Y axis in the horizontal position. By controlling the movement of the Y axis in the depositing process, a variable diameter part can be obtained. If the diameter of the part is changed, the rotating speed of the substrate will also be changed to keep the linear speed of the part constant. The substrate is made of a 6061 aluminium alloy with dimensions of $152 \times 152 \times 6.35$ mm.

2.3 Preheating and heat input control

When a temperature gradient exists in a body, the energy is transferred by conduction. The heat transfer rate per unit area is proportional to the normal temperature gradient:

$$\frac{q}{A} \sim \frac{\partial T}{\partial x} \tag{1}$$

When the proportionality constant is inserted,

$$q = -KA\left(\frac{\partial T}{\partial x}\right) \tag{2}$$

where

q = heat transfer rate
A = section area perpendicular to the direction of the heat flow
$\partial T/\partial x$ = temperature gradient in the direction of the heat flow
K = a positive constant which is called the thermal conductivity of the material

As shown in Fig. 4, the heat conductivity of aluminium is almost 6 times that of carbon steel and 12 times that of stainless steel. Suppose that q_0 is the suitable heat flow that ensures there is enough arc heat for the depositing process; all other conditions are equal except the materials. When aluminium is applied, the temperature gradient should be one-sixth that of carbon steel or one-twelfth that of stainless steel, and the preheating process must be applied in the depositing procedure of aluminium. The preheating process can reduce the temperature difference between the substrate and the depositing layers. In addition, the size of the 6061 aluminium alloy substrate is $152 \times 152 \times 6.35$ mm; it is very difficult to get a uniform molten pool at a welding speed of more than 70 mm/s using GTAW in a single pass.

In addition, as shown in Fig. 5, the first deposited layer L1 has the best heat conducting condition because the heat conducting area, the contacting area between the L1 layer and the substrate, is greater, and the path of the heat flow is shorter. The heat can be conducted to the substrate quickly and directly. When the height of the part increases, for example, the heat of the deposited layer Ln must be conducted through the previously

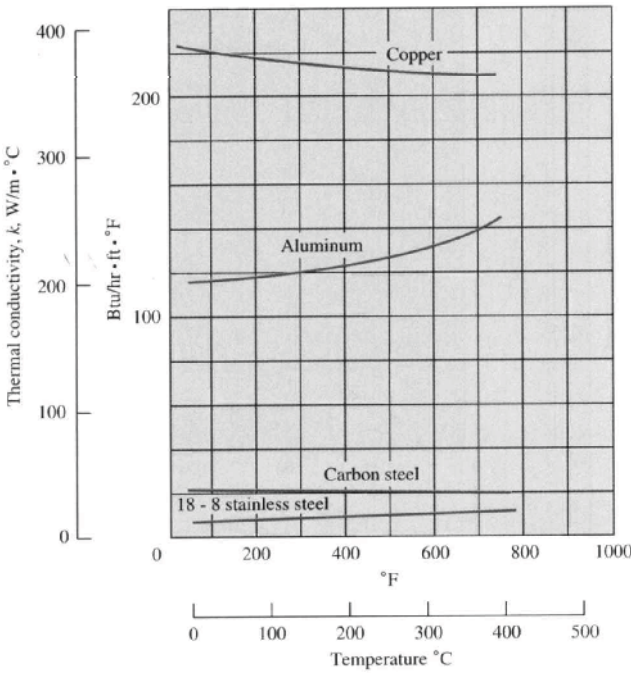

Fig. 4 Thermal conductivities of some typical metals (1 W/m °C = 0.5779 Btu/h ft °F) [**13**]

deposited layers, then to the substrate. The conductivity of air is less than 0.7 Btu/h ft °F and can be neglected. Compared with the L1 layer, the heat-conducting area is smaller, and the path of the heat flow is longer at the Ln layer. According to equation (2), q decreases with A and $\partial T/\partial x$ decreases. Therefore, more heat accumulates at the Ln layer than at the first L1 layer. When the heat accumulation is high enough, the previously deposited layers collapse, and the deposition process must be terminated. In order to overcome the problem, the heat input is reduced until a heat balance is established. Most importantly, it is possible to build parts without any additional cooling means.

2.4 Monitoring and controlling arc length

The arc length control is a key in the metal-depositing process. The reasons for this are as follows:

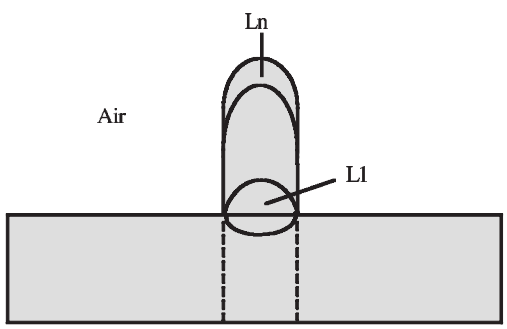

Fig. 5 Cross-section of the deposited layers on the substrate

1. The varying arc length is inevitable especially in a long-time deposition process.
2. The deposition process is not stable if the arc length cannot be kept constant because the varying arc length can result in a change to the heat input from the welding arc. The heat input from the welding arc Q is defined as

$$Q = \eta I V \tag{3}$$

where

η = coefficient of efficiency
I = welding current
V = arc voltage

The welding power source has a constant-current characteristic. Therefore, the fluctuation of the arc length causes the change in the arc voltage, V, and consequently, the heat input, Q, fluctuates as well.

3. In the experimental system, the wire-feeding guide is fixed to the welding torch. Therefore, the arc length is linked to the feed-wire position. The deposition process is not stable if the arc length cannot be kept constant because the variance of the arc length can result in an unstable transfer of the molten metal from the feed wire. The molten metal from the feed wire can be transferred to the molten pool very smoothly when the feed wire touches, with a suitable pressure, the surface of the substrate or the deposited layer. If the pressure is too high, there is a friction between the feed wire and the deposited layer surface, and the wire-feeding stability is interfered with. If the pressure is too low, the feed wire suspends in the welding arc, and the molten metal from the feed wire is discontinuously transferred to the molten pool by droplets. Both cases lead to an unstable transfer of the molten metal from the feed wire.

The images of the tungsten electrode, the welding arc, the filler wire and the deposited layers are shown in Fig. 6. The image processing steps are as follows:

Step 1: 3 × 3 noise average filtering. The intensity level of each pixel is replaced by the average of the surrounding pixel grey levels in the 3 × 3 filtering window.

Step 2: 3 × 3 edge enhancement. The algorithm is described as follows:

$$g(x, y) = m_{\mathrm{L}}(x, y) + k[f(x, y) - m_{\mathrm{L}}(x, y)] \tag{4}$$

where

$g(x, y)$ = enhanced grey level of pixel (x, y)
$f(x, y)$ = grey level of the pixel (x, y)
$m_{\mathrm{L}}(x, y)$ = average grey level of all the pixels in the window with pixel (x, y) as the central point
k = enhancement coefficient with a value greater than 1

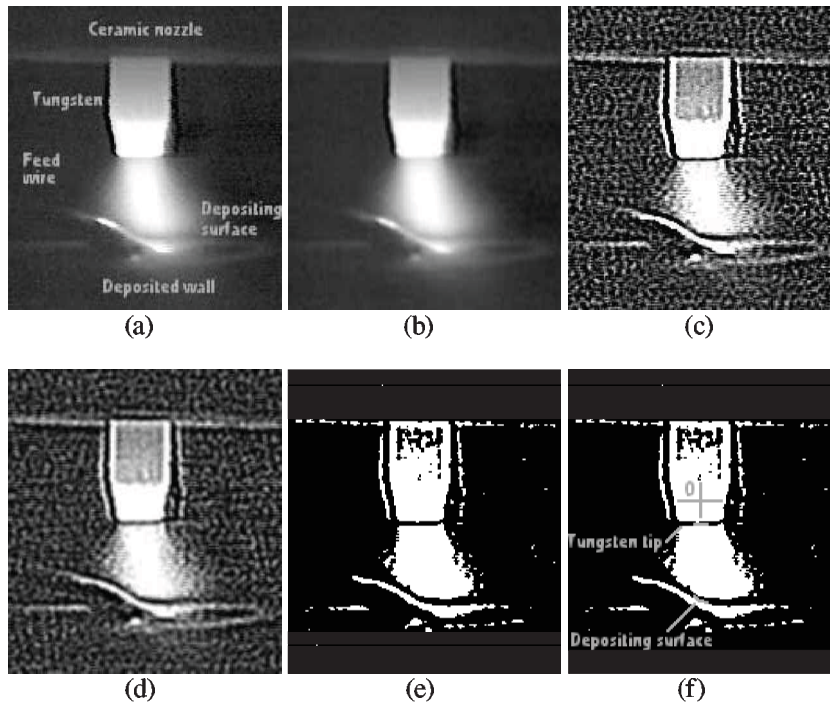

Fig. 6 Steps in image processing of arc length monitoring: (a) original image, (b) noise-filtered image, (c) edge-enhanced image, (d) noise-filtered image, (e) binary-value image, (f) edge-traced image

Step 3: 3×3 noise average filtering the same as step 1.
Step 4: binary image processing with a threshold of 150.
Step 5: arc length detection. Because of the relative position of the CCD camera and the fixed torch, point O on the tungsten electrode is static as shown in Fig. 6f. Point O is on the central line of the image of the tungsten electrode. Suppose that the original point of the image is on the upper left-hand corner, and the coordinate of point O is (i_O, j_O). Scanning is applied column by column in the range $j_O - 5$ to $j_O + 5$. On each column, scanning is taken from i_O to i_N, where i_N is the maximum row coordinate of the image. If the grey value of a pixel is zero, and the grey value of the next pixel is 255, the scanning pixel is along the edges. The distance between the first two detected pixels is considered as the arc length detection result. Eleven arc length detecting results can be obtained. In order to reduce the arc length detection error, an average value of the results is taken for the arc length. By calibration, 12 pixels in the image stand for 1 mm of the arc length; the detecting accuracy is 0.083 mm.

During the deposition of a layer, 15–30 images are acquired depending on the angular velocity of the part. The arc lengths are detected, and the average arc length is compared with the given arc length. At the beginning of the next layer, the movement of the Z' axis is controlled to keep the arc length to the given value.

3 RESULTS AND DISCUSSION

3.1 Preheating

The welding arc is used as the heat source. An infrared thermometer is used to monitor the temperature of the substrate in the preheating process. The temperature is acquired once during a revolution of the substrate at the same position. The sensing area on the substrate is round with a diameter of 20.0 mm. The location of the sensing area is shown in Fig. 7. The distance of O_1O_2 is 64 mm, where O_1 is the central point of the depositing path, and O_2 is the central point of the sensing area. The acquired temperature is an average temperature of

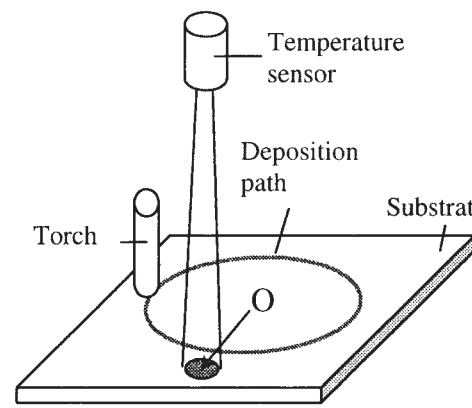

Fig. 7 Layout of sensing preheating temperature

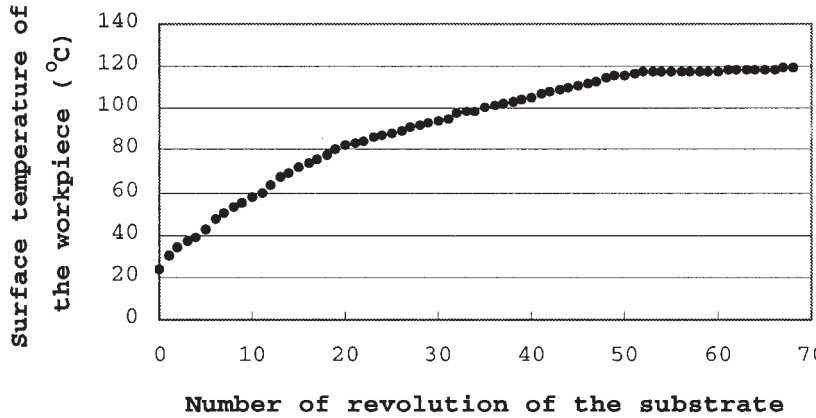

Fig. 8 Preheating temperature versus number of revolutions of substrate

the sensing area and is used to present the temperature of the substrate. As shown in Fig. 8, the temperature of the substrate is almost constant (118 °C) after preheating 52 revolutions; the welding current is 140 A, the angular speed of the substrate is 0.1 r/s (the welding speed depends on the diameter of the first layer of the part to be built). After 62 revolutions, there is a very noticeable distortion of the substrate that influences the temperature measurement of the substrate and so the preheating process must be terminated. Therefore, in this paper 118 °C is the target temperature of the preheating process with the substrate of a 6061 aluminium alloy, $152 \times 152 \times 6.35$ mm. With temperature monitoring, the deposition process begins when the temperature of the substrate reaches 118 °C. The preheating temperature mainly depends on the size of the substrate. In general, the larger the substrate size, the higher the required preheating temperature. This is because the heat conductivity of aluminium is very high. The larger substrate has a bigger heat sink than the smaller substrate when the preheating temperature is the same.

3.2 Relationship between the geometry of the deposited layer and the welding parameters

The shape and dimensions of the weld bead are very important in the use of the rapid prototyping system based on deposition by a welding technique, because these factors determine the limits of the wall thickness that can be built and influence the quality of the surface finish. Numerous experiments are undertaken to build single-weld beads for a range of welding conditions. The main welding parameters that are varied include the welding current, the welding-arc voltage, the welding speed and the wire-feed speed. The welding current and arc voltage are monitored. Subsequently, the sizes (height and width) of the built weld bead are measured. When one of the main welding parameters increases, the others are kept constant. A large amount of data are generated in this way and the general trends are shown in Table 1.

The heat input is directly proportional to the product of welding current and welding arc voltage and inversely proportional to welding speed. Therefore, the relationship between the bead width and the heat input is directly proportional. The bead height is inversely proportional to the heat input and directly proportional to the wire feeding speed.

The bead width is inversely proportional to the wire feeding speed but the experimental results show that the wire feeding speed has a very small effect on the bead width. The wire feeding speed can change the bead width by affecting the heat input. Melting the filler metal consumes the welding arc energy, the higher the wire feeding speed, the lower the heat input. However, the consumed energy is a very small fraction of the welding arc energy and can be neglected. Variations in the rate of filler metal applied to the weld result in different arc lengths (and hence different arc voltages);

Table 1 General relationship of weld bead sizes and welding parameters

	Effect on variables*			
Increasing welding variables	Welding current	Welding arc voltage	Bead width	Bead height
Welding current	↑	↑	↑	↓
Welding arc voltage	=	↑	↑	↓
Welding speed	=	↓	↓	↑
Wire feeding speed	=	↓	↓	↑

* =, no effect; ↑, increasing; ↓, decreasing.

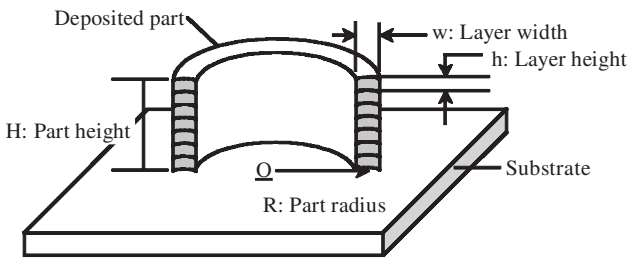

Fig. 9 Sketch of deposited part

this in turn directly affects the heat input. However, if arc length control is applied this effect can also be neglected. Therefore, the bead width only depends on the heat input. Through experiments with different heat inputs and wire feeding speeds the relationship between the bead width and the heat input can be obtained. If the bead width is determined, the heat input is also fixed. In this case the bead height only depends on the wire feeding speed.

The definition of the geometrical sizes of the built parts is shown in Fig. 9. Abbreviations are: w, width of the deposited layer; h, height of the deposited layer; H, height of the finished part; R, radius of the finished part; O, central point of the finished part. The wire feeding speed is determined by

$$v_{\text{wire}} = \frac{\omega R w h}{\pi r^2} \tag{5}$$

where

v_{wire} = wire feeding speed
r = radius of the feeding wire
ω = angular speed of the substrate

The different layer heights can be obtained by changing the wire feeding speed as calculated according to equation (5). The deposition parameters also need to be optimized based on the required dimensional accuracy and surface quality.

3.3 Test parts

The first test part is in the form of a cylinder as shown in Fig. 10. The part is to be built of 300 layers with a layer height, width and diameter of 0.4, 4.1 and 101.6 mm respectively. The main process parameters are as follows: arc length, 5 mm; welding speed, 80 mm/s; heat input control is realized by reducing the welding current from 140 to 100 A in the first 40 layers with a speed of 1 A/layer while keeping the welding current at 100 A for the rest of the layers. The results of the deposition process are:

1. The height is 116.0 mm.
2. The width is 4.2 mm.
3. The diameter is 102.0 mm.
4. The error of the part height is 3.3 per cent.
5. The error of the part width is 2.4 per cent.
6. The error of the part diameter is 1.0 per cent.
7. The average of the surface roughness, R_a is 2.45–2.77 μm.

The second test part is in the form of a cone as shown in Fig. 11. The part is to be built in two segments: the first segment includes 60 layers with a diameter of 76.0 mm; the second segment includes 100 layers with a beginning diameter of 76.0 mm and an ending diameter of 46.0 mm. Both of the two segments have the same layer height of 0.4 mm and a layer width of 5.0 mm. The main process parameters are as follows: arc length, 5 mm; welding speed, 80 mm/s; heat input control is realized by reducing the welding current from 150 to 110 A in the first 40 layers with a speed of 1 A/layer while keeping the welding current at 110 A for the rest of the layers. The results of the deposition process are:

1. The height is 66.0 mm.
2. The width is 4.9 mm at the first segment and 5.3 mm at the second segment.
3. The diameter is 75.5 mm at the first segment and 47.0 mm at the end of the second segment.

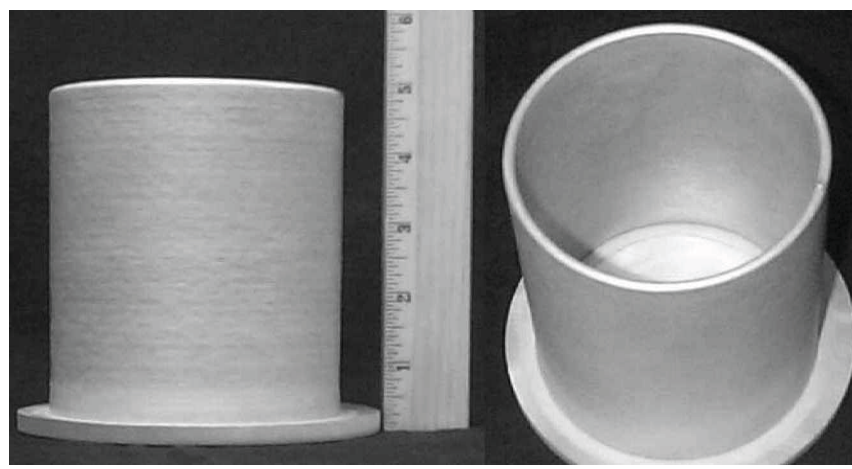

Fig. 10 Part in form of cylinder

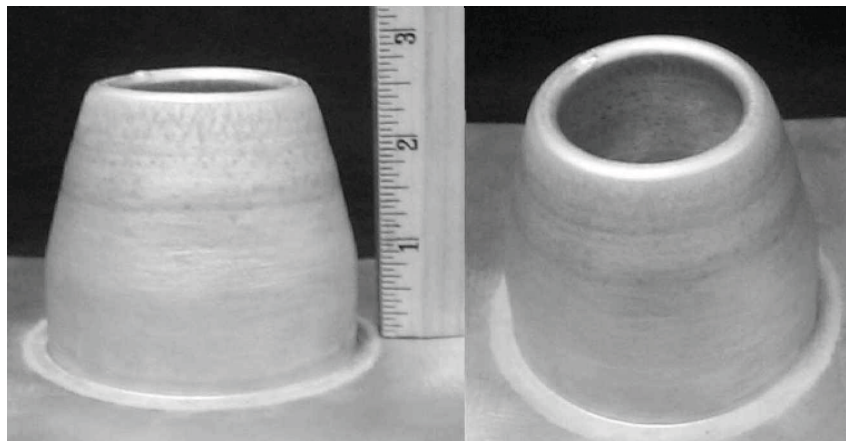

Fig. 11 Part in form of cone

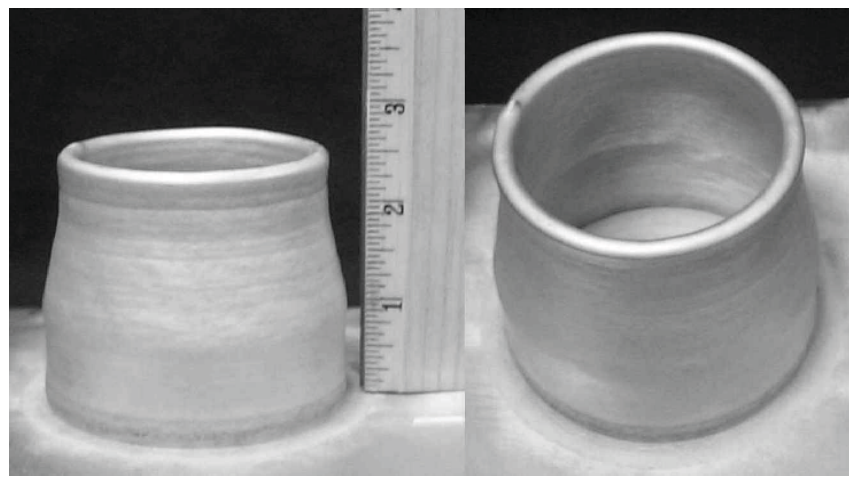

Fig. 12 Part in form of pipe reducer

4. The error of the part height is 3.1 per cent.
5. The error of the maximum width of the part is 6.0 per cent.
6. The error of the maximum diameter of the part is 2.2 per cent.
7. The average of the surface roughness, R_a, is 1.76–2.17 μm.

The third test part is in the form of a pipe reducer as shown in Fig. 12. The part is to be built in three segments: the first segment includes 80 layers with a diameter of 76.0 mm; the second segment includes 60 layers with a beginning diameter of 76.0 mm and an ending diameter of 64.0 mm; the third segment includes 20 layers with a diameter of 64.0 mm. All three segments have the same layer height of 0.4 mm and layer width 4.6 mm. The main process parameters are as follows: arc length, 5 mm; welding speed, 70 mm/s; heat input control is realized by reducing the welding current from 140 to 100 A in the first 40 layers with a speed of 1 A/layer while keeping the welding current at 100 A for the rest of the layers. The results of the deposition process are:

1. The height is 65.1 mm.
2. The width is 4.5 mm at the first segment, 4.6 mm at the second segment and 4.8 mm at the third segment.
3. The diameter is 75.5 mm at the first segment and 65.5 mm at the third segment.
4. The error of the part height is 1.7 per cent.
5. The error of the maximum width of the part is 4.3 per cent.
6. The error of the maximum diameter of the part is 2.3 per cent.
7. The average of the surface roughness, R_a, is 2.36–2.99 μm.

4 CONCLUSION

There are three important issues that have to be addressed in the design of the deposition process based on variable polarity gas tungsten arc welding: the preheating of the substrate, the arc-length monitoring and controlling, and the heat-input controlling. This process allows the cylindrical components to be directly and

successfully built of an aluminium alloy. Several parts were made with perfectly acceptable surface quality, mechanical properties and accurate dimensions. This process can be used to produce samples of variable thickness, but cannot yet be used to produce asymmetric samples.

ACKNOWLEDGEMENTS

The authors would like to give special thanks to Dr F. Wang and M. Valant for support in this research work. The work was financially supported by THECB (Texas Higher Education Coordinating Board) Grants 003613-0005-1997 and 003613-0022-1999, NSF (National Science Foundation) Grants DMI-9732848 and DMI-9809198 and by a US Department of Education Grant P200A80806-98.

REFERENCES

1 **Kassmaul, K., Schoch, F. W.** and **Lucknow, H.** High quality large components 'shape welded' by a SAW process. *Weld. J.*, September 1983.

2 **Piehl, K.-H.** Formgebendes Schweißen von Schwekomponenten. Company report, January 1989 (Thyssen Aktiengesellschaft, Duisburg).

3 **Doyle, T. E.** Shape melting technology. In the Third International Conference on *Desktop Manufacturing: Making Rapid Prototyping Pay Back*, *The Management Round Table*, October 1991 (Babcock and Wilcox, Cambridge, Massachusetts).

4 **Dickens, P. M., Cobb, R., Gibson, I.** and **Pridham, M. S.** Rapid prototyping using 3D welding. *J. Des. and Mfg*, 1993, **3**.

5 **Ribeiro, A. F.** and **Norrish, J.** Metal based rapid prototyping for more complex shapes. In Proceedings of the 6th Biennial International Conference on *Computer Technology in Welding*, Lanaken, Belgium, 9–12 June 1996 (TWI, Abington Publishing).

6 **Ribeiro, A. F.** and **Norrish, J.** Rapid prototyping process using metal directly. In Proceedings of the 7th Annual Solid Freeform Fabrication Symposium, Austin, Texas, 12–14 August 1996.

7 **Ribeiro, A. F.** and **Norrish, J.** Making components with controlled metal deposition. In IEEE International Symposium on *Industrial Electronics*, Guimaraes, Portugal, 7–11 July 1997.

8 **Kovacevic, R.** and **Beardsley, H. E.** Process control of 3D welding as a droplet-based rapid prototyping technique. In Proceedings of the 9th Annual Solid Freeform Fabrication Symposium, Austin, Texas, 10–12 August 1998.

9 **Beardsley, H. E.** and **Kovacevic, R.** Controlling heat input and metal transfer for 3D welding-based rapid prototyping. In Proceedings of the 5th International Conference on *Trends in Welding Research*, Pine Mountain, Georgia, 1–5 June 1998.

10 **Song, Y., Park, S., Hwang, K., Choi, D.** and **Jee, H.** 3D welding and milling for direct prototyping of metallic parts. In Proceedings of the 9th Annual Solid Freeform Fabrication Symposium, Austin, Texas, 10–12 August 1998.

11 **Karunakaran, K., Shanmuganathan, P., Roth-Koch, S.** and **Koch, U.** Direct rapid prototyping of tools. In Proceedings of the 9th Annual Solid Freeform Fabrication Symposium, Austin, Texas, 10–12 August 1998.

12 **O'Brien, R. L.** Welding process. In *Welding Handbook*, Vol. 2, 8th edition, 1991 (American Welding Society, Miami, Florida).

13 **Holman, J. P.** *Heat Transfer*, 8th edition, 1997 (McGraw-Hill, New York).